

# Differential gut microbiota and inflammatory cytokines contribute to IgA vasculitis

Y. Chen<sup>1,2</sup>, Y. Zeng<sup>2,3</sup>, Y. Zhang<sup>2,3</sup>, J. Chen<sup>1,2</sup>, Y. Qian<sup>1,2</sup>, J. Huang<sup>1,2</sup>,  
G. Chen<sup>1,2</sup>, G. Xia<sup>1,2</sup>, C. Wang<sup>1,2</sup>, A. Feng<sup>2</sup>, X. Nie<sup>1,2,3</sup>

<sup>1</sup>Department of Paediatrics, Fuzong Clinical Medical College of Fujian Medical University, Fuzhou;

<sup>2</sup>Department of Paediatrics, 900th Hospital of PLA Joint Logistic Support Force, Fuzhou;

<sup>3</sup>Department of Paediatrics, Dongfang Hospital of Xiamen University, School of Medicine, Xiamen University, Fuzhou, China.

---

## Abstract

### Objective

Immunoglobulin A vasculitis (IgAV) is the most common form of vasculitis in childhood. Emerging evidence indicates that gut microbiota plays a key role in the pathogenesis of IgAV. However, the factors linking gut microbiota to the onset and progression of IgAV are poorly understood. We aimed to demonstrate that the presence of a specific dysbiosis in patients with IgAV contributes to the onset of IgAV.

---

### Methods

We transplanted gut microbiota from human donors with IgAV or healthy controls (HCs). The changes in gut microbiota and serum indexes of the recipient mice were detected, and the IgAV-associated bacteria were determined by integrating the results from the mouse sequence data analysis with the human sequence results.

---

### Results

55 amplicon sequence variants (ASVs) specific to IgAV children were detected in the recipient IgAV microbiota (rIMb) mice, and 35 ASVs specific to healthy children were detected in the recipient healthy microbiota (rHMb) mice. Gut microbiota in rIMb mice differs from that in rHMb mice. Alcaligenaceae could discriminate rIMb from rHMb mice, while its abundance was decreased in rIMb compared to rHMb ( $p < 0.05$ ). In children with IgAV, the abundance of Burkholderiaceae (Alcaligenaceae accounted for 99.7%) at the family level was significantly lower compared to HCs, which can be used to distinguish children with IgAV from HCs, and the constructed receiver operating characteristic (ROC) curve had an area under the curve (AUC) value of 0.766. In addition, the rIMb group had a markedly higher interleukin (IL)-17A and IL-21 level than those in the rHMb group. The Spearman correlation analysis indicated significant correlations between the relative levels of these pro-inflammatory cytokines, IgA and alterations of gut microbiota.

---

### Conclusion

IgAV is characterised by disturbances of gut microbiota composition and an imbalance in inflammatory cytokines. The manipulation of gut microbiota could be a possible way to prevent and manage IgAV.

---

### Key words

IgA vasculitis, gut microbiota, IgA-inducing cytokines, IgA

Yi Chen, MM\*  
 Yuguang Zeng, MM\*  
 Yuanzhen Zhang, MM  
 Junyan Chen, MM  
 Yifang Qian, MM  
 Jun Huang, MM  
 Guangming Chen, MD  
 Guizhi Xia, MD  
 Chengfeng Wang, MM  
 Ai Feng, BM  
 Xiaojing Nie, MD

\*Contributed equally.

Please address correspondence to:  
 Xiaojing Nie  
 Department of Paediatrics,  
 900th Hospital of PLA Joint Logistic  
 Support Force,  
 350025 Fuzhou, China.  
 E-mail: searchnj051@126.com

Received on August 4, 2024; accepted in  
 revised form on October 28, 2024.

© Copyright CLINICAL AND  
 EXPERIMENTAL RHEUMATOLOGY 2025.

*Funding: this work was supported in part by the National Natural Science Foundation of China (81300583); Science and Technology Innovation Project of Fujian Province (2019Y9043); Key Project of Social Development of Fujian Province of China (2019Y0069); Key Project of Social Development of Fujian Province of China (2023Y0068); Foundation of the 900th Hospital of Joint Logistic Support Force (2021MS15, 2021JQ10, 2022MS30, 2022ZD05, 2023QN02).*

*Competing interests: none declared.*

## Introduction

Immunoglobulin A vasculitis (IgAV), the most common form of vasculitis in childhood, is characterised by inflammation in small vessels caused by perivascular deposition of IgA1-dominant immune complexes (1, 2). Patients with IgAV exhibit variable clinical symptoms, including non-thrombocytopenic palpable purpura, abdominal pain, arthritis/arthralgia, and renal involvement (3). Although the precise pathogenic mechanisms of IgAV have yet to be fully elucidated, several studies have highlighted the significance of gut microbiota in its pathogenesis (4–8). However, the factors connecting gut microbiota to the onset and progression of IgAV are poorly understood.

Abnormal IgA1 glycosylation, resulting in the production of galactose-deficient IgA1 (Gd-IgA1), underlies the pathogenesis of IgAV (9). Nevertheless, the source and mechanisms of Gd-IgA1 production remain unclear. Previous studies have demonstrated that the circulating Gd-IgA1 in IgAV patients partly originated from the mucosa (10–12). Additional evidence suggests that gut microbiota participate in the regulation of IgA synthesis. Specifically, gut microbiota contributes to increasing IgA production, and microbial infections in the intestine promote the class switch of naive B-cells to IgA antibody-secreting cells, via both T-cell-independent and T-cell-dependent pathways (13). Thus, it can be inferred that gut microbiota is implicated in the pathogenesis of IgAV by activating the intestinal mucosal immune system and eventually participating in the regulation of IgA synthesis.

In this study, we aimed to demonstrate that a specific dysbiosis in patients with IgAV contributes to disease onset by using a murine model transplanted with human gut microbiota.

## Materials and methods

### Human faecal samples collection

The study protocol was approved by the Ethics Committee of 900th Hospital of PLA Joint Logistic Support Force (NO: 2019-009). All subjects had given written informed consent. All the human data were derived from our pre-

vious study (8). The inclusion criteria for IgAV were based on previous literature (3, 14). In total, 16 IgAV subjects (relapsing IgAV) and 23 healthy controls (HCs) were recruited from 900th Hospital of PLA Joint Logistic Support Force, the Fujian Provincial Maternity and Children's Hospital, Fujian Provincial Hospital, and Fujian Medical University Union Hospital (Table I). Participants who were treated with antibiotics, immunosuppressors, proton pump inhibitors, chemotherapy, and radiotherapy within 2 weeks before faecal collection, and who were with allergic rhinitis, allergic asthma, allergic cough and other diseases that could affect the results of the study were excluded. The middle part of stools from each subject was collected with disposable sterile containers and stored at -80°C before sequencing (strictly adhered to the national standard: GB/T 41908-2022).

### Animal experiments

All animal experiments were approved by the Ethics Committee of the 900th Hospital of PLA Joint Logistic Support Force (no.: 2020-73). The specific pathogen-free (SPF) mice were bred in the Laboratory Animal Center at 900th Hospital of PLA Joint Logistic Support Force. All mice were maintained at an ambient temperature of 20°C–26°C, and humidity of 40–70%, at a cycle of 12 hours light & 12 hours dark, and had free access to the autoclaved rodent diet and autoclaved water.

To prepare the faeces for faecal microbiota transplantation (FMT), five samples from children with IgAV (relapsing IgAV) and five samples from HCs were selected and mixed at equal weights. All five children with relapsing IgAV exhibited palpable purpura and renal involvement. Then we diluted a mixed human faecal sample (1 g) in 10 mL of saline and filtered through a filter mesh to remove residues. The faecal material was centrifuged for 3 min at 5000 rpm, and 200 µL of the supernatant was introduced by gavage into each recipient mouse. Mice were handled once every day for 3 days. Faecal samples were collected before and 7 days after FMT, and immediately stored at -80°C. Sera

were obtained via cardiac puncture on day 7 following the FMT.

#### IgA and cytokines analyses

Levels of IgA, B cell activating factor (BAFF), interleukin (IL)-1 $\beta$ , IL-6, IL-17A, IL-21, and tumour necrosis factor-alpha (TNF- $\alpha$ ) in the sera of mice were measured by Mouse IgA ELISA Kits (MULTI SCIENCES, China), Mouse BAFF ELISA Kits (MULTI SCIENCES, China), Mouse IL-1 $\beta$  ELISA Kits (MULTI SCIENCES, China), Mouse IL-6 ELISA Kits (MULTI SCIENCES, China), Mouse IL-17A ELISA Kits (MULTI SCIENCES, China), Mouse IL-21 ELISA Kits (MULTI SCIENCES, China), and Mouse TNF- $\alpha$  ELISA Kits (MULTI SCIENCES, China).

#### Faecal DNA extraction, polymerase chain reaction (PCR) amplification, and 16S rRNA gene amplicon sequencing

Total genomic DNA samples were extracted using the OMEGA Soil DNA Kit (M5635-02) (Omega Bio-Tek, Norcross, GA, USA), following the manufacturer's instructions, and stored at -20°C prior to further analysis. The quantity and quality of extracted DNAs were measured using a NanoDrop NC2000 spectrophotometer (Thermo Fisher Scientific, Waltham, MA, USA) and agarose gel electrophoresis, respectively.

PCR amplification of the bacterial 16S rRNA genes V3-V4 region was performed using the forward primer 338F (5'-ACTCCTACGGGAG-GCAGCA-3') and the reverse primer 806R (5'-CGGACTACHVGGGT-WTCTAAT-3'). Sample-specific 7-bp barcodes were incorporated into the primers for multiplex sequencing. The PCR components contained 5  $\mu$ L of buffer (5 $\times$ ), 0.25  $\mu$ L of Fast pfu DNA Polymerase (5 U/ $\mu$ L), 2  $\mu$ L (2.5 mM) of dNTPs, 1  $\mu$ L (10 uM) of each Forward and Reverse primer, 1  $\mu$ L of DNA Template, and 14.75  $\mu$ L of ddH<sub>2</sub>O. Thermal cycling consisted of initial denaturation at 98°C for 5 min, followed by 25 cycles consisting of denaturation at 98°C for 30 s, annealing at 53°C for 30 s, and extension at 72°C for 45 s, with a final extension of 5 min at 72°C.

**Table I.** Clinical characteristics of the human subjects.

Characteristics	IgAV	HCS	p-value
Sample size	16	23	-
Female, n (%)	10 (62.5%)	10 (43.5%)	0.709
Age, median (IQR)	6.0 (5.0~9.0)	9.0 (6.2~11.4)	0.097

IgAV: IgAV patients; HCS: healthy controls.

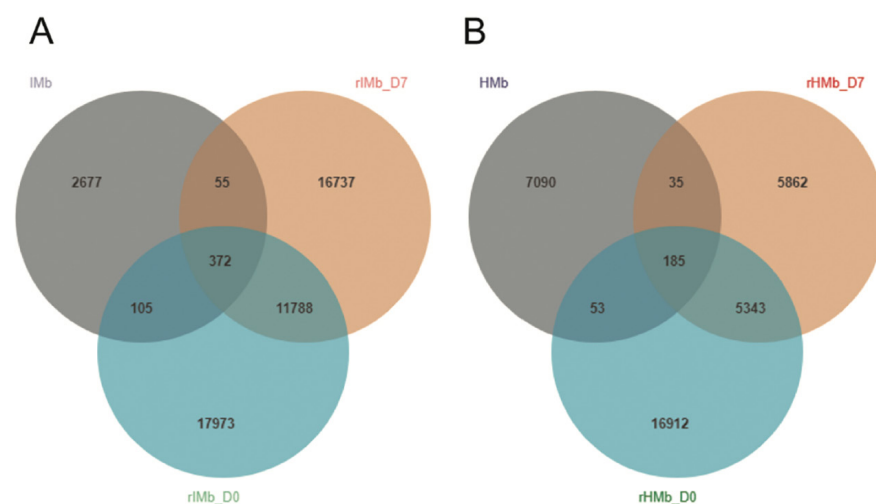


**Fig. 1.** Venn diagrams representing the colonisation of donor ASVs in the recipient mice.

**A:** 55 ASVs specific to IgAV children (grey circle) were detected in the rIMb mice (the blue circle represents the mice before being colonised with IgAV microbiota, and the orange circle represents the mice colonised with IgAV microbiota after 7 days).

**B:** 35 ASVs specific to healthy children (grey circle) were detected in the rHMb mice (the blue circle represents the mice before being colonised with healthy microbiota, and the orange circle represents the mice colonised with healthy microbiota after 7 days).

IMb: IgAV microbiota; HMb: healthy microbiota; rIMb: recipient of IgAV microbiota; rHMb: recipient of healthy microbiota.

PCR amplicons were purified with Vazyme VAHTSTM DNA Clean Beads (Vazyme, Nanjing, China) and quantified using the Quant-iT PicoGreen ds-DNA Assay Kit (Invitrogen, Carlsbad, CA, USA). After the individual quantification step, amplicons were pooled in equal amounts, and pair-end 2 $\times$ 250 bp sequencing was performed using the Illumina NovaSeq platform with NovaSeq 6000 SP Reagent Kit (500 cycles) at Shanghai Personal Biotechnology Co., Ltd (Shanghai, China).

Microbiome bioinformatics were performed with QIIME2 2019.4 with slight modification according to the official tutorials (<https://docs.qiime2.org/2019.4/tutorials/>). Briefly, raw sequence data were demultiplexed using the demux plugin following by primers cutting with cutadapt plugin. Sequences were then quality filtered, denoised, merged and chimera removed using the

DADA2 plugin. Non-singleton amplicon sequence variants (ASVs) were aligned with mafft and used to construct a phylogeny with fasttree2. Taxonomy was assigned to ASVs using the classify-sklearn naïve Bayes taxonomy classifier in feature-classifier plugin against the gg\_13 Database.

Sequence data analyses were mainly performed using QIIME2 and R packages (v3.2.0). The taxonomy compositions and abundances were visualised using MEGAN and GraPhlAn. Venn diagram was generated to visualise the shared and unique ASVs among samples or groups using R package "VennDiagram", based on the occurrence of ASVs across samples/groups regardless of their relative abundance. Taxa abundances at the ASV levels were statistically compared among samples or groups by MetagenomeSeq. Random forest analysis was applied to

discriminating the samples from different groups using QIIME2 with default settings. Nested stratified k-fold cross validation was used for automated hyperparameter optimisation and sample prediction. The number of k-fold cross-validations was set to -2.

**Statistics**

Statistical analysis was performed using SPSS v. 24.0 (SPSS, Chicago, IL, US) and R (v. 4.1.2). Data were analysed for homogeneity of variance and normal distribution. The independent sample t-test was used for comparison between groups for measurement data obeying normal distribution and satisfied homogeneity of variance, all expressed as ( $\bar{x} \pm s$ ). Mann-Whitney U-tests were performed for the data that failed to meet normal distribution or homogeneity of variance, all presented by median (interquartile range [IQR]). The counting data was tested using chi-square test. *p*-values <0.05 were considered to indicate statistical significance.

**Results**

*Transplantation of human microbiota from children with IgAV and healthy children to recipient mice*

To determine whether the human gut microbiota can be transmissible to mice by FMT, faecal matter from children with IgAV and healthy children was transplanted to SPF mice. Mice colonised with IgAV microbiota (IMb) and healthy microbiota (HMb) were labeled as recipient IMb (rIMb) and recipient HMb (rHMb), respectively. Mixed faeces rather than single faeces from 5 children with IgAV or 5 healthy children were used to ensure the homogeneity. A total of 6,932,568 sequences were obtained from 64 samples, with 6,059,747 sequences after denoising by DADA2. On average, 94,683 sequences per sample were acquired and were shown to have a mean sequence of 418bp (range, 15–435bp). Venn diagrams were generated to visualise the establishment of the donor ASVs in mice, which revealed the specific gut microbiota of humans could colonise the intestinal tract of mice (Fig. 1). 55 ASVs specific to IgAV children were

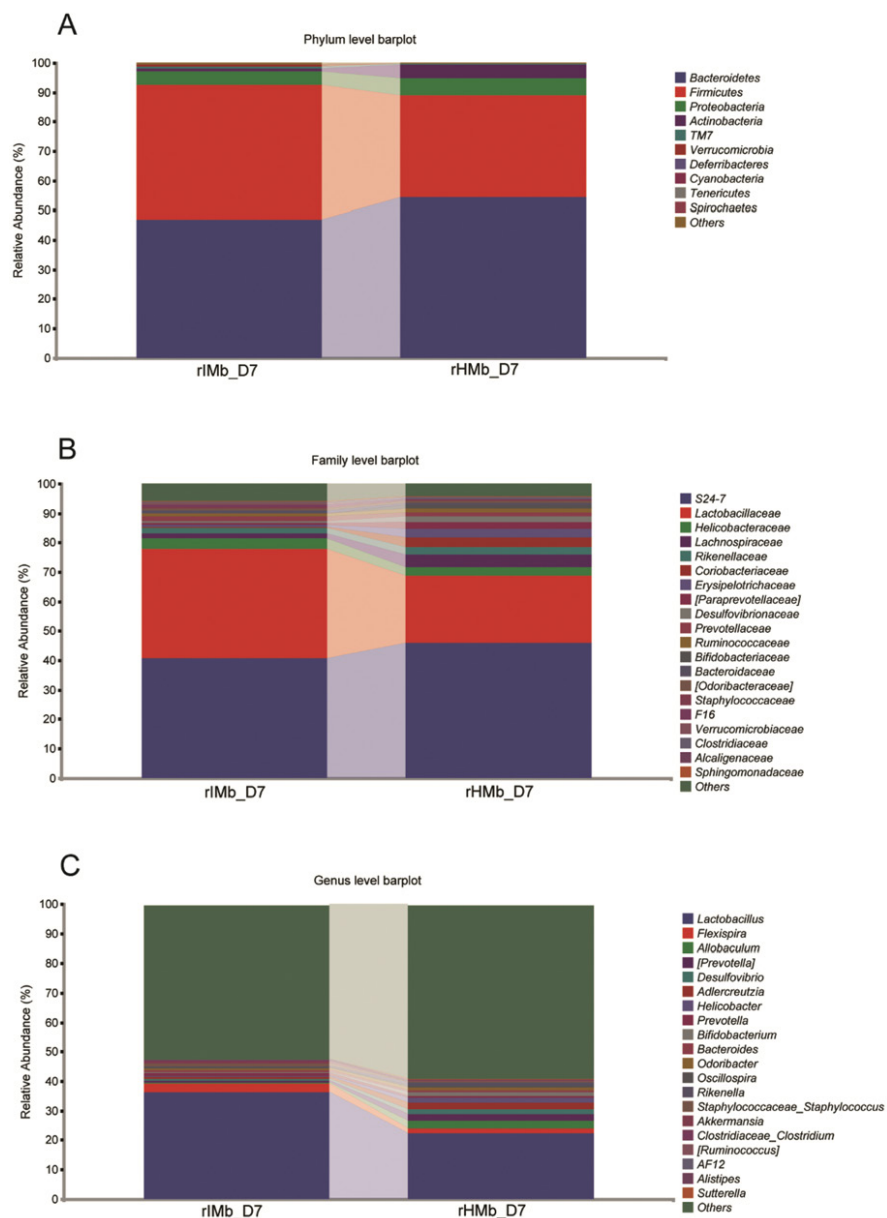


**Fig. 2.** Comparison relative taxa abundance between rHMb and rIMb. **A:** Relative abundance of dominant phylum in the rHMb and rIMb. **B:** Relative abundance of dominant family in the rHMb and rIMb. **C:** Relative abundance of dominant genus in the rHMb and rIMb. rIMb: recipient of IgAV microbiota; rHMb: recipient of healthy microbiota.

detected in the rIMb, and 35 ASVs specific to healthy children were detected in the rHMb.

*Gut microbiota in rIMb mice differed from that in rHMb mice*

After FMT, the differences in the bacterial community structure were evident in recipient mice (Fig. 2 and Supplementary Table S1-S3). At the phylum level, the relative abundance of *Firmicutes* in rIMb was higher than that in rHMb. In contrast, the relative abundance of *Bacteroidetes*, *Proteobac-*

*teria*, and *Actinobacteria* were lower than those in rHMb, with the difference in *Actinobacteria* being considered significant (*p*<0.05). At the family level, *Lactobacillaceae* was more abundant in rIMb compared with rHMb, while the abundances of S24-7, *Helicobacteraceae*, *Lachnospiraceae*, *Rikenellaceae*, *Coriobacteriaceae* were decreased in rIMb compared with rHMb. The difference in *Coriobacteriaceae* abundance between these two groups was considered significant (*p*<0.05). At the genus level, the relative abundance of

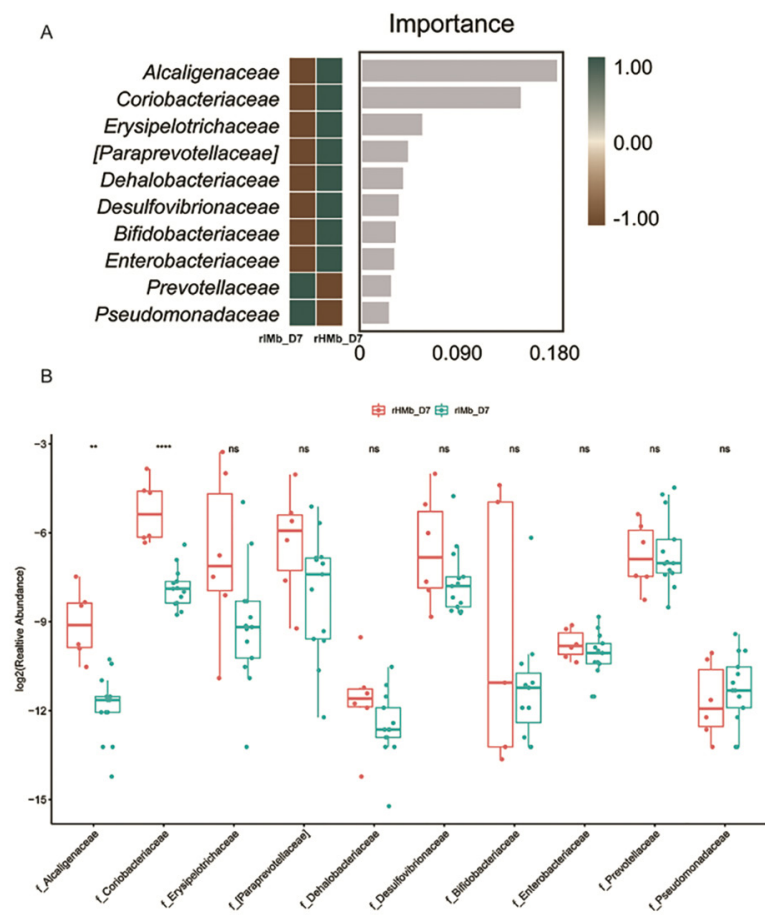


**Fig. 3.** Microbial signatures of discriminating rIMb and rHMb from each other at the family level.

**A:** Random Forests analysis identified 10 bacterial families used to differentiate rIMb from rHMb. **B:** Relative abundance of 10 bacterial families in rIMb and rHMb at 7 days after FMT.

rIMb: recipient of IgAV microbiota; rHMb: recipient of healthy microbiota; ns: no significant difference.

Significance was accepted at  $p < 0.05$ .

\* $p < 0.05$ , \*\* $p < 0.01$ , \*\*\* $p < 0.001$ , \*\*\*\* $p < 0.0001$ .

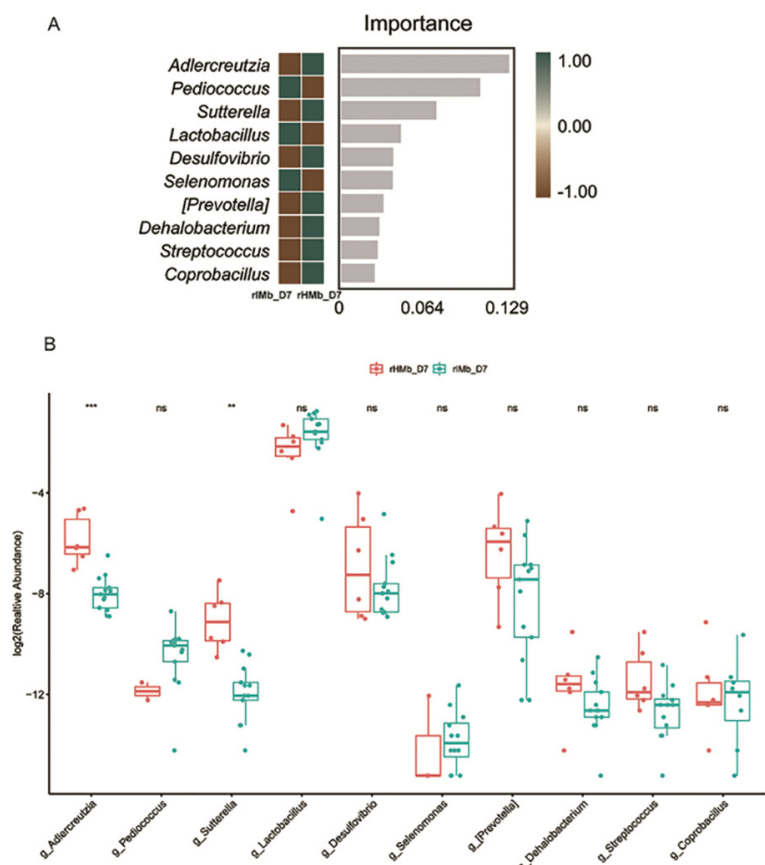


**Fig. 4.** Microbial signatures of discriminating rIMb and rHMb from each other at the genus level.

**A:** Random Forests analysis identified 10 bacterial genera used to differentiate rIMb from rHMb. **B:** Relative abundance of 10 bacterial genera in rIMb and rHMb at 7 days after FMT.

rIMb: recipient of IgAV microbiota; rHMb: recipient of healthy microbiota; ns: no significant difference.

Significance was accepted at  $p < 0.05$ .

\* $p < 0.05$ , \*\* $p < 0.01$ , \*\*\* $p < 0.001$ , \*\*\*\* $p < 0.0001$ .

**Table II.** The importance score of Random Forests analysis at the family level.

Family	Importance score
<i>Alcaligenaceae</i>	0.180
<i>Coriobacteriaceae</i>	0.146
<i>Erysipelotrichaceae</i>	0.055
[ <i>Prevotellaceae</i> ]	0.042
<i>Dehalobacteriaceae</i>	0.038
<i>Desulfovibrionaceae</i>	0.034
<i>Bifidobacteriaceae</i>	0.031
<i>Enterobacteriaceae</i>	0.030
<i>Prevotellaceae</i>	0.027
<i>Pseudomonadaceae</i>	0.025

**Table III.** The importance score of Random Forests analysis at the genus level.

Genus	Importance score
<i>Adlercreutzia</i>	0.129
<i>Pediococcus</i>	0.107
<i>Sutterella</i>	0.073
<i>Lactobacillus</i>	0.046
<i>Desulfovibrio</i>	0.040
<i>Selenomonas</i>	0.040
[ <i>Prevotella</i> ]	0.032
<i>Dehalobacterium</i>	0.029
<i>Streptococcus</i>	0.028
<i>Coprobacillus</i>	0.026

*Lactobacillus* in rIMb was higher than that in rHMb, while the relative abundance of [*Prevotella*], *Allobaculum*, *Desulfovibrio*, *Adlercreutzia* were lower than those in rHMb. The difference in *Adlercreutzia* abundance between these two groups was also considered significant ( $p < 0.05$ ).

*Gut microbiota biomarker for discriminating rIMb from rHMb mice*

To identify microbial signatures for discriminating rIMb from rHMb, we used a supervised machine learning technique, called Random Forests, to identify discriminative bacterial families and genera between the two groups. Furthermore, Random Forests also assigned an importance score to each predictor (15, 16). The Random Forests analysis showed that *Alcaligenaceae* played a key role in the pathogenesis of IgAV (Fig. 3-4). We identified 10 bacterial families used to differentiate rIMb from rHMb (Fig. 3A), and eight of them presented a decreased abundance in rIMb compared to rHMb. Specifically, the abundance of *Alcaligenaceae* (importance score = 0.180) (Table II) and *Coriobacteriaceae* (importance score = 0.146) (Table

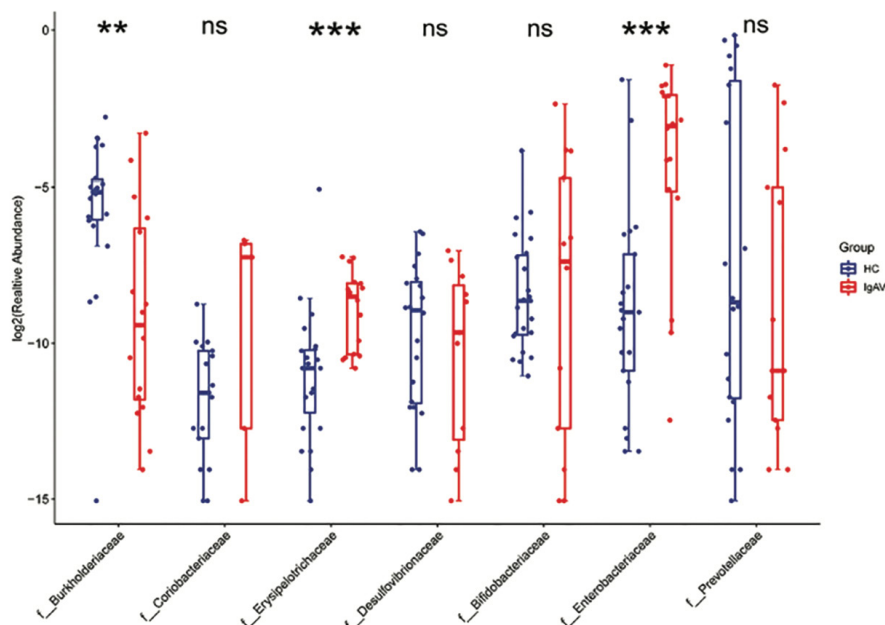


**Fig. 5.** Relative abundance of 10 bacterial families in IgAV patients and HCs. Significance was accepted at  $p < 0.05$ . \* $p < 0.05$ , \*\* $p < 0.01$ , \*\*\* $p < 0.001$ , \*\*\*\* $p < 0.0001$ , ns means no significant difference. IgAV: children with IgAV; HCs: healthy controls.

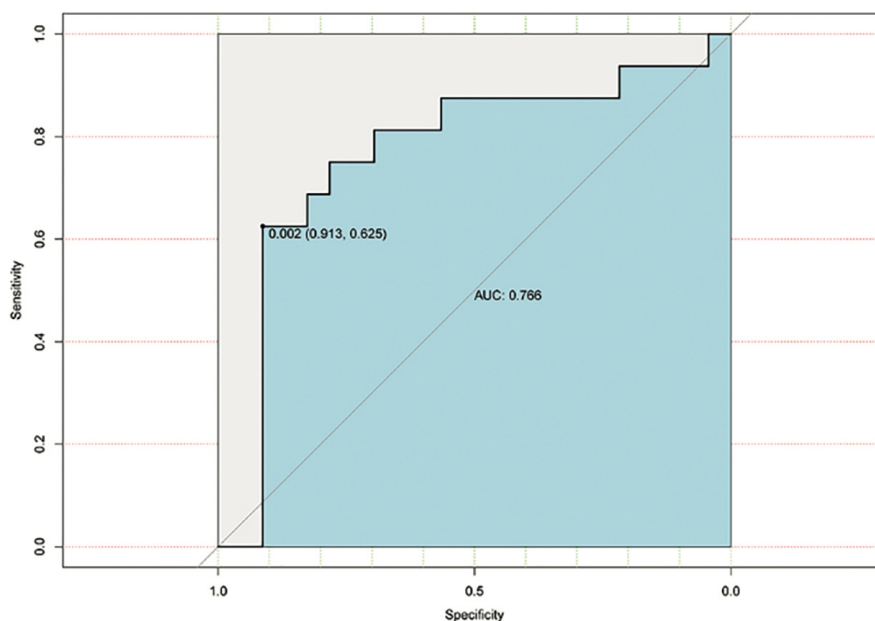


**Fig. 6.** The ROC curve of *Burkholderiaceae*. ROC curves showed that *Burkholderiaceae* enabled discriminating IgAV patients and HCs from each other, with high diagnostic accuracy (AUC=0.766).

II) was significantly lower in rIMb than in rHMb ( $p < 0.05$ ) (Fig. 3B). Moreover, we also identified 10 bacterial genera that can differentiate rIMb from rHMb. Compared to rHMb mice, the rIMb mice were characterised by 7 decreased genera (Fig. 4A), whereas *Adlercreutzia* (importance score = 0.129) (Table III) and *Sutterella* (importance score

= 0.073) (Table III) were the two most significant contributors among these ( $p < 0.05$ ) (Fig. 4B).

*Validation of IgAV-associated bacteria in human samples*

To assess the newly identified microbial biomarkers above, a relative abundance analysis for the differential 10

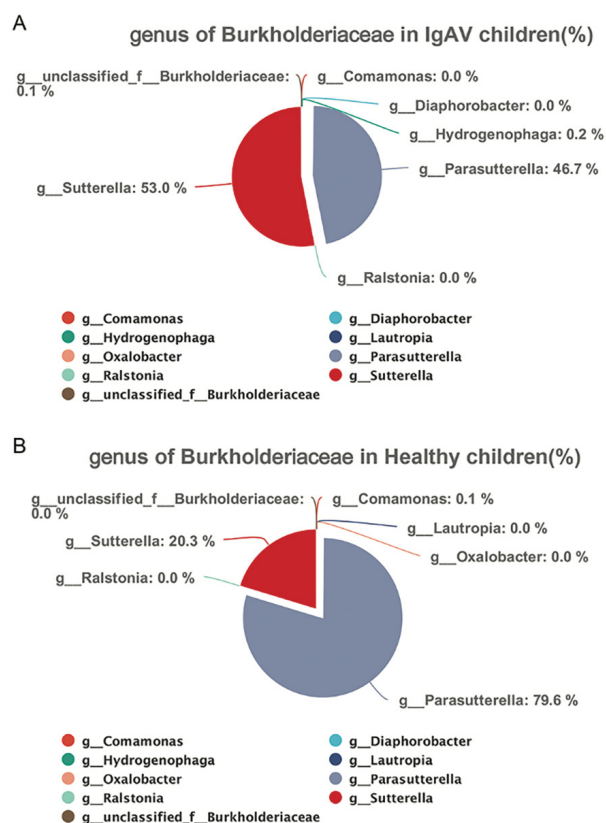


**Fig. 7.** The composition of *Burkholderiaceae* in human subjects. **A:** The composition of *Burkholderiaceae* in faeces of children with IgAV. **B:** The composition of *Burkholderiaceae* in faeces of healthy children.

bacterial families screened in mice was performed in human samples. Totally, 16 children with IgAV and 23 HCs were recruited from our previous study (8). The detailed clinical characteristics of these subjects were presented in Table I. There were no significant differences in age or sex between the two groups. The box plot showed that the abundance of *Burkholderiaceae* in IgAV subjects was significantly lower at the family level compared with HCs subjects (Fig. 5), while that of *Erysipelotrichaceae* and *Enterobacteriaceae* were enriched in IgAV subjects (due to the difference in the annotation system, the bacteria categorised under *Alcaligenaceae* families like *Sutterella* and *Parasutterella* were classified as *Burkholderiaceae* in human samples). To identify and quantify the diagnostic potential of *Alcaligenaceae* in IgAV, receiver operating characteristic (ROC) curves were performed. It was found that *Burkholderiaceae* could be used to discriminate IgAV subjects from HCs subjects, with high diagnostic accuracy (area under the curve [AUC = 0.766]) (Fig. 6). Meanwhile, the specificity and sensitivity were 91.3% and 62.5%, respectively. In addition, we also observed that *Sutterella* and *Parasutterella* accounted for the highest fraction of the *Burkholderiaceae* in human subjects, with the total of the two accounting for 99.7% of IgAV subjects and 99.9% of HCs subjects, respectively (Fig. 7).

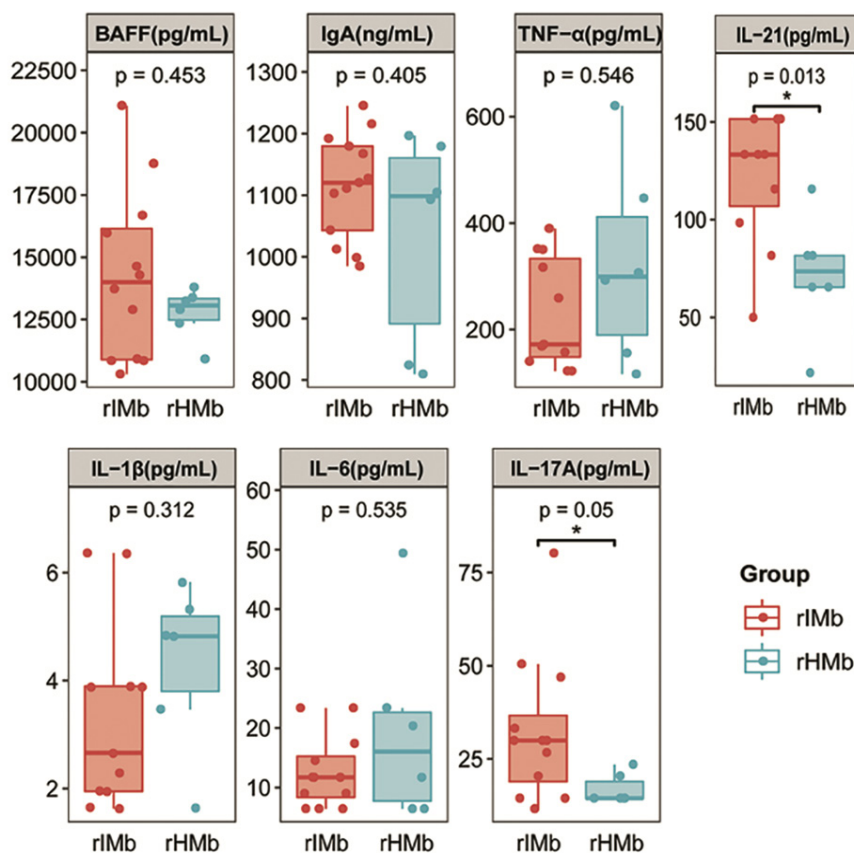


**Fig. 8.** Serum indexes levels exhibited by rIMb mice and rHMB mice. rIMb: recipient of IgAV microbiota; rHMB: recipient of healthy microbiota. Significance was accepted at  $p < 0.05$ . \* $p < 0.05$ .

*Analysis of the serum index levels in rIMb mice and rHMB mice*

Compared to the rHMB group, the rIMb group had significantly higher levels of serum IgA, BAFF, IL-17A, and IL-21. In contrast, the rIMb group had markedly lower levels of serum TNF- $\alpha$ , IL-1 $\beta$ , and IL-6 than those in the rHMB group. The differences in the levels of IL-17A and IL-21 between the groups were statistically significant ( $p < 0.05$ ) (Fig. 8).

*Correlation analysis between gut microbiota and serum indexes*

The potential correlation between the gut microbiota and serum indexes including IgA, BAFF, IL-1 $\beta$ , IL-6, IL-

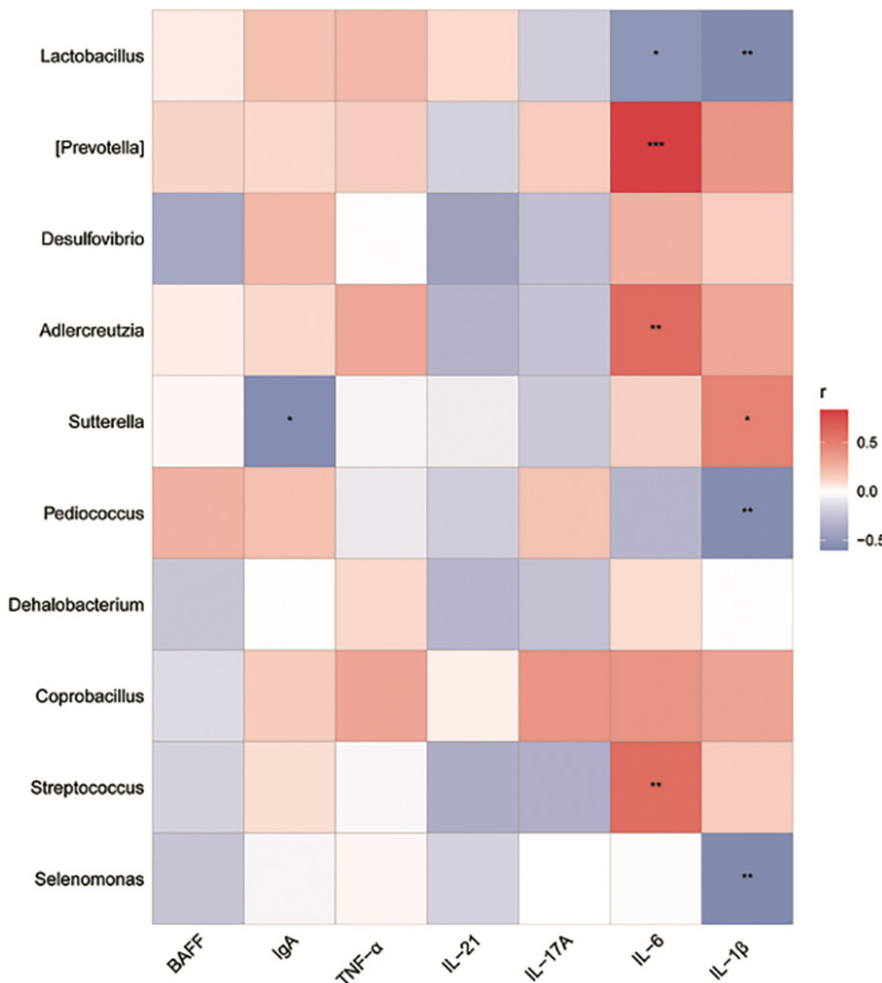


**Fig. 9.** Heatmap of correlations between gut microbiota and serum indexes. Positive correlation is in red, negative correlation is in blue. Significance was accepted at  $p < 0.05$ . \* $p < 0.05$ , \*\* $p < 0.01$ , \*\*\* $p < 0.001$ .

17A, IL-21, and TNF- $\alpha$  were analysed (Fig. 9). The results showed that the abundance of *Lactobacillus* was negatively correlated with IL-1 $\beta$  ( $r = -0.59$ ,  $p = 0.008$ ) and IL-6 ( $r = -0.52$ ,  $p = 0.023$ ). The abundance of *[Prevotella]* was positively correlated with IL-6 ( $r = 0.82$ ,  $p < 0.001$ ), and IL-6 was also positively correlated with the abundance of *Adlercreutzia* ( $r = 0.60$ ,  $p = 0.006$ ) and *Streptococcus* ( $r = 0.60$ ,  $p = 0.007$ ). The abundance of *Pediococcus* ( $r = -0.58$ ,  $p = 0.009$ ) and *Selenomonas* ( $r = -0.59$ ,  $p = 0.008$ ) was negatively correlated with IL- $\beta$ . Moreover, the abundance of *Sutterella* was positively correlated with IL-1 $\beta$  ( $r = 0.47$ ,  $p = 0.041$ ), negatively correlated with IgA ( $r = -0.57$ ,  $p = 0.011$ ), but not significantly correlated with IL-17 ( $r = -0.21$ ,  $p > 0.05$ ) and IL-21 ( $r = -0.07$ ,  $p > 0.05$ ). There was no significant difference in the correlation

between the serum IgA level and the abnormal levels of cytokines in recipient mice (Fig. 10).

### Discussion

Recent studies have manifested a close correlation between the gut microbiota and IgAV (4-8). Nevertheless, whether the alterations in gut microbiota constitute a cause or a consequence of the disease remains unknown. To determine the role of gut microbiota in the pathogenesis of IgAV, the initial step involves screening and analysing the differential gut microbiota between children with IgAV and healthy controls. This will furnish us with preliminary understandings of the disease's mechanisms (17). Subsequently, an animal model of IgAV is indispensable for validating these findings. However, an acceptable animal model is current-

ly unavailable. FMT is a powerful and effective approach for the construction of human flora-associated (HFA) animals (18). Through faecal transplant experiments, we found that some specific microbiota, which contribute to the synthesis of IgA via intestinal mucosal immunity, are involved in the pathogenesis of IgAV.

Other researchers have demonstrated that this microbiota transplant strategy was beneficial for investigating the mechanism of microbiota in disease development, including inflammatory bowel disease (IBD), autism spectrum disorder (ASD), myasthenia gravis (MG), obesity, and so forth (19-22). Although the strategy of using mixed faecal samples for the preparation of faecal microbiota suspension might pose challenges in terms of standardisation due to the differences in microbial composition among donors, which could result in increased variability in experimental results (23). However, multiple donor samples can better represent the general population's gut microbiota, which is crucial for studies aiming to understand the broader implications of gut microbiota on health and disease. The use of mixed faecal samples from multiple donors can enhance the HFA mice model's ability to represent the complexity of the human gut microbiota by reducing the biological variability associated with a single donor (24). Furthermore, this approach has been validated by multiple relevant studies (25-27). Therefore, we opted to use mixed faecal samples from multiple donors, ensuring uniform quality in the mixture, to prepare the faecal microbiota suspension. Since previous clinical observations have confirmed that relapses in children with IgAV are associated with diverse bacterial infections (28, 29). Additionally, our previous studies have demonstrated that there exist differences in the gut microbiota among children with IgAV, whether it is their first episode or a relapse, and healthy children. Nevertheless, the relapsing IgAV group exhibits a more pronounced dysbiosis, with a notable increase in the abundance of *Proteobacteria* (8). We hold the view

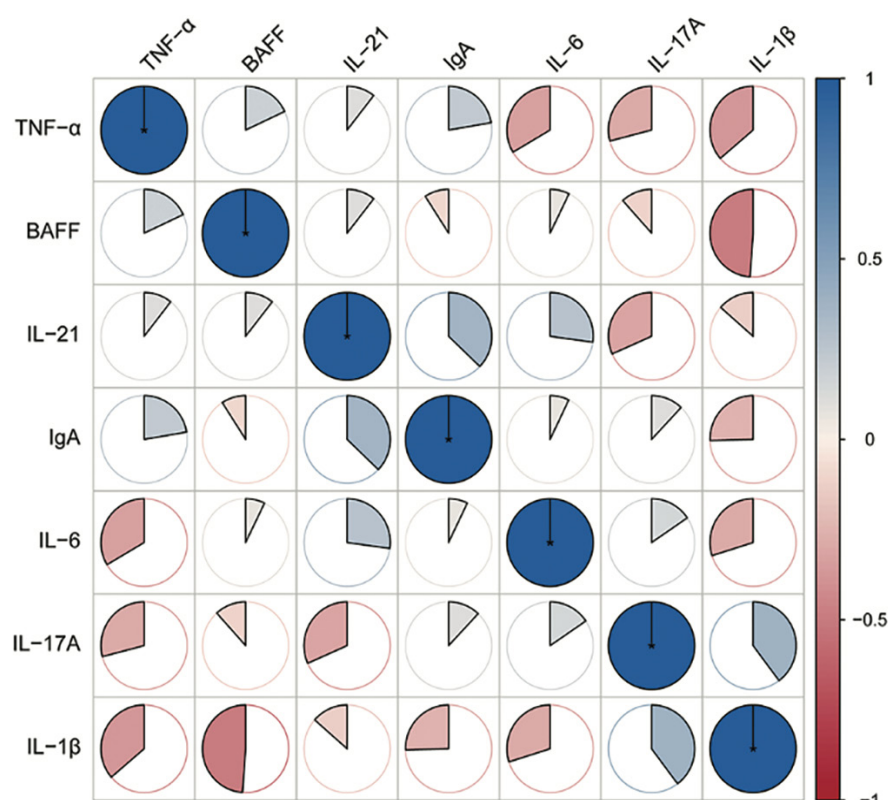


**Fig. 10.** Spearman correlation analysis of serum IgA and serum cytokines level. Positive correlation is in blue, negative correlation is in red. Significance was accepted at  $p < 0.05$ , \* $p < 0.05$ .

that the gut microbiota of children with relapsing IgAV is more representative, given that the disease duration in children with relapsing IgAV is usually longer. Here, we compared the gut microbiota profiles between the mice colonised with relapsing IgAV microbiota and those with healthy microbiota after FMT. The findings revealed that the microbiota composition of rIMb was substantially different from that of rHMB. For example, our findings showed that compared with rHMB, the relative abundance of *Actinobacteria* was significantly decreased in rIMb.

We further identified a family of bacteria that was significantly and specifically associated with IgAV. Compared to rIMb individuals, the family *Alcaligenaceae* was enriched in rHMB subjects, suggesting its potential in differentiating rIMb and rHMB, with an importance score of 0.180. Interestingly, we found that the *Burkholderiaceae* was also enriched in HCs subjects (the family *Alcaligenaceae* accounted for 99.9%). Additionally, ROC analysis

indicated that the *Burkholderiaceae* could serve as a potential biomarker for distinguishing children with IgAV from HCs, as evidenced by an AUC of 0.766. *Alcaligenaceae* is a gram-negative bacterium that belongs to the phylum *Proteobacteria*, class *Betaproteobacteria*, and order *Burkholderiales*. Evidence shows that this bacterium contributes to various allergic diseases, such as asthma, atopic dermatitis (AD), and so forth, yet the mechanisms remain unclear (30, 31). Wang *et al.* (30) reported that the relative abundance of the *Alcaligenaceae* family was significantly lower in the high-IgE asthma (HEA) group compared to the low-IgE asthma (LEA) group. The potential mechanism was that *Alcaligenaceae* could lead to the imbalance between T-helper cell (Th) 1 and Th2 immune responses. IgAV is considered to be associated with allergies. Additionally, some evidence suggests that the imbalance of Th cell differentiation and subsequent cytokine dysregulation is implicated in IgAV disease (32-34). In our study, we found that the abundance

of *Alcaligenaceae* was significantly decreased in rIMb. This result suggests that *Alcaligenaceae* might be related to the pathogenesis of IgAV through a complex mechanism, which demands further exploration. Moreover, our results demonstrate that this strategy is an effective approach for constructing IgAV flora-associated animals.

*Sutterella* is one of the most vital species within the *Alcaligenaceae* family and is associated with the degradation of IgA (35, 36). Moon *et al.* (37) reported that mice characterised by low faecal IgA levels were attributed to the high abundance of *Sutterella* within the gut microbiota. Through *in vitro* experiments, they also confirmed that live bacteria and bacterial lysates could degrade both the free and bound secretory component (SC) of IgA, while the addition of a broad-spectrum protease inhibitor cocktail partially prevented SC degradation. Moreover, compared with the mice characterised by high faecal IgA, the mice with low faecal IgA exhibited increased distal colon ulceration upon exposure to dextran sulphate sodium (DSS)-induced injury (37). Thus, these findings revealed that *Sutterella* itself and its lysates were associated with the impairment of intestinal mucosal immune responses through reducing the IgA level in intestinal mucosal and ultimately inducing inflammation. Similarly, we observed that *Sutterella* was significantly decreased in rIMb, which could be used to distinguish rIMb from rHMB (the importance score was 0.073). Given the IgA-degrading characteristics of *Sutterella*, we hypothesised that the IgA level in rIMb increased due to the decrease of IgA degradation. In this study, we detected higher level of IgA in the serum samples of rIMb. Meanwhile, we performed a Spearman correlation analysis to determine the potential correlation between *Sutterella* and serum IgA. Accordingly, we found that IgA levels were negatively associated with *Sutterella* in recipient mice. Hence, the *Sutterella* might be involved in the pathogenesis of IgAV through the IgA degradation pathway. It is necessary to note that there was no significant difference in the serum IgA

levels between different recipient mice. Thus, further *in vitro* experiments are still required to investigate the monotonic relationships between *Sutterella* and serum IgA levels.

Research on various types of systemic vasculitis has demonstrated that specific cytokines might be intricately linked to the onset of these disease onset (38, 39). Likewise, IgAV is associated with dysregulations in the levels of inflammatory cytokines, some of which facilitate the synthesis of IgA and contribute to organ impairment, while others enhance proinflammatory effects in a subset of IgAV patients. Given the substantial significance of Gd-IgA1 in the pathogenesis of IgAV, cytokines capable of inducing IgA synthesis, such as BAFF, IL-17A, and IL-21, are of particular interest to us (40-43). Furthermore, clinical studies on IgAV have suggested that inflammation-related cytokines like IL-1 $\beta$ , IL-6, and TNF- $\alpha$  could serve as biomarkers for diagnosing IgAV, indicating their partial contribution to the initiation of IgAV. (44-47). Observing the variation in the levels of these cytokines in the serum of recipient mice and correlating them with IgA and gut microbiota can assist in uncovering the interactions among cytokines, IgA, and gut microbiota, and how they jointly influence the progression of IgAV. To this end, we revealed the differences in cytokine levels between serum samples from different recipient mice and conducted a correlation analysis with IgA, which might provide mechanistic insights into IgAV. For instance, we found higher levels of IL-17A and IL-21 in the sera of rIMb than in rHMb, suggesting the gut microbiota profile in children with IgAV affects the expression of IL-17A and IL-21 in the serum samples of recipient mice. Importantly, previous studies have explored that IL-17 and IL-21 were the upstream regulators of IgA synthesis, and the two differentially regulated intestinal IgA response in a synergetic manner (43, 48). IL-17 regulated the intestinal IgA response through stimulating the expression of polymeric Ig receptor (PIgR) in intestinal epithelial cells, whereas IL-21 promoted IgA-secreting B cells and B cell IgA produc-

tion by inducing B cell IgA class switch recombination (CSR) directly (43, 48). However, in our model, the correlation between the cytokines and IgA was not significant, suggesting that IL-17A and IL-21 were not the most predominant upstream regulators of serum IgA.

In addition to the aforementioned, we observed a positive correlation between the abundance of *Sutterella* and the serum level of IL-1 $\beta$  in recipient mice. This is of special interest as IL-1 $\beta$  is a pro-inflammatory cytokine released by various immune modulating cells belonging to the IL-1 family, which causes disruption of the intestinal tight junction (TJ) barrier by increasing TJ permeability (49). Li *et al.* (50) observed that dietary resveratrol attenuated colitis symptoms and ameliorated colonic tissue damage in DSS-treated mice, and even partially ameliorated gut microbiota dysbiosis induced by DSS. Specifically, resveratrol effectively decreased the abundance of genera including *Sutterella*, and down-regulated the expression of pro-inflammatory cytokines including IL-1 $\beta$  in the colon of DSS-treated mice. A Pearson's correlation analysis indicated a significant positive correlation between the abundance of *Sutterella* and the level of IL-1 $\beta$ . This indicated that the abundance of *Sutterella* might promote gut mucosal inflammation due to an increase in the expression of inflammatory cytokines, such as IL-1 $\beta$ . Additional evidence is available that IL-1 $\beta$  is a potent inducer of IgA synthesis. For instance, IL-1 $\beta$  knockout (KO) mice show a significant decrease in small intestinal IgA cells and reduced intestinal IgA levels (51), inhibition of IL-1 $\beta$  signalling on intestinal epithelial cells blocks the IgA tissue deposition in *Lactobacillus casei* cell wall extract (LCWE) -induced Kawasaki disease (KD) vasculitis mice (52), and IL-1 receptor antagonist partially prevented the progression of spontaneously occurring IgA nephropathy in mice (53). Together, we deduced that in our model, an increase in the abundance of *Sutterella* might affect the expression of IL-1 $\beta$ , thereby promoting intestinal inflammation and IgA synthesis.

In summary, we identified gut microbiota specific to IgAV, and provided

evidence that disturbances in the gut microbiota profile and imbalance in inflammatory cytokines might contribute to the onset of IgAV. Some possible mechanisms underlying the onset of IgAV supported by our data are as follows: i) the degradation of IgA was reduced by decreasing the abundance of IgA-degrading bacteria, including *Sutterella*; ii) the production of IgA was enhanced by increasing the potent inducer of IgA synthesis, including IL-1 $\beta$ , IL-17A, and IL-21, which were affected by gut microbiota dysbiosis; iii) an elevated serum IgA ultimately involved in the pathogenesis of IgAV. This study provides new insight into the pathogenesis of IgAV, and opens new possibilities for further exploration of gut microbiota-based strategies used for the treatment of IgAV.

This study has the following limitations: i) we had only a limited number of donors in each group and the intervention period was short. Therefore, future studies with more human donors are needed; ii) due to the lack of human blood samples, human tissue samples, and mice tissue samples, how gut microbiota influences blood signatures and tissue injury remains unclear. Further studies integrating the faecal and blood signatures are valuable for a profound understanding of the microbial function in IgAV.

### Acknowledgments

The authors greatly appreciate all the efforts made by the hospital staff in recruiting and treating patients. We thank the Laboratory Animal Centre at 900th Hospital of PLA Joint Logistic Support Force for the smooth conduct of the experiment and generous participation in our research effort.

### References

1. DAVIN J-C, COPPO R: Henoch-Schönlein purpura nephritis in children. *Nat Rev Nephrol* 2014; 10(10): 563-73. <https://doi.org/10.1038/nrneph.2014.126>
2. OZEN S, SAG E: Childhood vasculitis. *Rheumatology* (Oxford). 2020; 59 (Suppl 3): iii95-iii100. <https://doi.org/10.1093/rheumatology/kez599>
3. OZEN S, PISTORIO A, IUSAN SM *et al.*: EULAR/PRINTO/PRES criteria for Henoch-Schönlein purpura, childhood polyarteritis nodosa, childhood Wegener granulomatosis

- and childhood Takayasu arteritis: Ankara 2008. Part II: Final classification criteria. *Ann Rheum Dis* 2010; 69(5): 798-806. <https://doi.org/10.1136/ard.2009.116657>
4. LI M, WANG X, LIN X *et al.*: Comparison and analysis of gut microbiota in children with IgA vasculitis with different clinical symptoms. *Front Pediatr* 2021; 9: 800677. <https://doi.org/10.3389/fped.2021.800677>
  5. TAN J, ZHONG Z, TANG Y, QIN W: Intestinal dysbiosis featuring abundance of Streptococcus associates with Henoch-Schönlein purpura nephritis (IgA vasculitis with nephritis) in adult. *BMC Nephrol* 2022; 23(1): 10. <https://doi.org/10.1186/s12882-021-02638-x>
  6. WANG X, ZHANG L, WANG Y *et al.*: Gut microbiota dysbiosis is associated with Henoch-Schönlein Purpura in children. *Int Immunopharmacol* 2018; 58: 1-8. <https://doi.org/10.1016/j.intimp.2018.03.003>
  7. WEN M, DANG X, FENG S *et al.*: Integrated analyses of gut microbiome and host metabolome in children with Henoch-Schönlein Purpura. *Front Cell Infect Microbiol* 2021; 11: 796410. <https://doi.org/10.3389/fcimb.2021.796410>
  8. ZHANG Y, XIA G, NIE X *et al.*: Differences in manifestations and gut microbiota composition between patients with different henoch-schönlein purpura phenotypes. *Front Cell Infect Microbiol* 2021; 11: 641997. <https://doi.org/10.3389/fcimb.2021.641997>
  9. SUGINO H, SAWADA Y, NAKAMURA M: IgA vasculitis: etiology, treatment, biomarkers and epigenetic changes. *Int J Mol Sci* 2021; 22(14): 7538. <https://doi.org/10.3390/ijms22147538>
  10. KANEKO F, MORI N, MIURA Y: Secretory IgA in Schönlein-Henoch purpura. *Dermatologica* 1984; 169(5): 318-23. <https://doi.org/10.1159/000249619>
  11. LOMAX-SMITH JD, ZABROWARNY LA, HOWARTH GS, SEYMOUR AE, WOODROFFE AJ: The immunochemical characterization of mesangial IgA deposits. *Am J Pathol* 1983; 113(3): 359-64.
  12. MOJA P, QUESNEL A, RESSEGUIER V *et al.*: Is there IgA from gut mucosal origin in the serum of children with Henoch-Schönlein purpura? *Clin Immunol Immunopathol* 1998; 86(3): 290-97. <https://doi.org/10.1006/clin.1997.4493>
  13. HE J-W, ZHOU X-J, LV J-C, ZHANG H: Perspectives on how mucosal immune responses, infections and gut microbiome shape IgA nephropathy and future therapies. *Theranostics* 2020; 10(25): 11462-78. <https://doi.org/10.7150/thno.49778>
  14. CALVO-RÍO V, HERNÁNDEZ JL, ORTIZ-SANJUÁN F *et al.*: Relapses in patients with Henoch-Schönlein purpura: analysis of 417 patients from a single center. *Medicine* (Baltimore). 2016; 95(28): e4217. <https://doi.org/10.1097/md.00000000000004217>
  15. KNIGHTS D, COSTELLO EK, KNIGHT R: Supervised classification of human microbiota. *FEMS Microbiol Rev* 2011; 35(2): 343-59. <https://doi.org/10.1111/j.1574-6976.2010.00251.x>
  16. YATSUNENKO T, REY FE, MANARY MJ *et al.*: Human gut microbiome viewed across age and geography. *Nature* 2012; 486(7402): 222-27. <https://doi.org/10.1038/nature11053>
  17. HU X, FAN R, SONG W *et al.*: Landscape of intestinal microbiota in patients with IgA nephropathy, IgA vasculitis and Kawasaki disease. *Front Cell Infect Microbiol* 2022; 12: 1061629. <https://doi.org/10.3389/fcimb.2022.1061629>
  18. WOS-OLLEY M, BLEICH A, OXLEY APA *et al.*: Comparative evaluation of establishing a human gut microbial community within rodent models. *Gut Microbes* 2012; 3(3): 234-49. <https://doi.org/10.4161/gmic.19934>
  19. JANG H-M, KIM J-K, JOO M-K *et al.*: Transplantation of fecal microbiota from patients with inflammatory bowel disease and depression alters immune response and behavior in recipient mice. *Sci Rep* 2021; 11(1): 20406. <https://doi.org/10.1038/s41598-021-00088-x>
  20. SHARON G, CRUZ NJ, KANG D-W *et al.*: Human gut microbiota from autism spectrum disorder promote behavioral symptoms in mice. *Cell* 2019; 177(6): 1600-18. <https://doi.org/10.1016/j.cell.2019.05.004>
  21. ZHENG P, LI Y, WU J *et al.*: Perturbed microbial ecology in myasthenia gravis: evidence from the gut microbiome and fecal metabolome. *Adv Sci* (Weinh) 2019; 6(18): 1901441. <https://doi.org/10.1002/advs.201901441>
  22. RIDAURA VK, FAITH JJ, REY FE *et al.*: Gut microbiota from twins discordant for obesity modulate metabolism in mice. *Science* 2013; 341(6150): 1241214. <https://doi.org/10.1126/science.1241214>
  23. PARK JC, IM S-H: Of men in mice: the development and application of a humanized gnotobiotic mouse model for microbiome therapeutics. *Exp Mol Med* 2020; 52(9): 1383-96. <https://doi.org/10.1038/s12276-020-0473-2>
  24. ZHOU W, CHOW K-H, FLEMING E, OH J: Selective colonization ability of human fecal microbes in different mouse gut environments. *ISME J* 2019; 13(3): 805-23. <https://doi.org/10.1038/s41396-018-0312-9>
  25. LI B, GUO K, ZENG L *et al.*: Metabolite identification in fecal microbiota transplantation mouse livers and combined proteomics with chronic unpredictable mild stress mouse livers. *Transl Psychiatry* 2018; 8(1): 34. <https://doi.org/10.1038/s41398-017-0078-2>
  26. ZHENG P, ZENG B, LIU M *et al.*: The gut microbiome from patients with schizophrenia modulates the glutamate-glutamine-GABA cycle and schizophrenia-relevant behaviors in mice. *Sci Adv* 2019; 5(2): eaau8317. <https://doi.org/10.1126/sciadv.aau8317>
  27. WONG SH, ZHAO L, ZHANG X *et al.*: Gavage of fecal samples from patients with colorectal cancer promotes intestinal carcinogenesis in germ-free and conventional mice. *Gastroenterology* 2017; 153(6): 1621.33.e6. <https://doi.org/10.1053/j.gastro.2017.08.022>
  28. MARRO J, WILLIAMS C, PAIN CE, ONI L: A case series on recurrent and persisting IgA vasculitis (Henoch Schönlein purpura) in children. *Pediatr Rheumatol Online J* 2023; 21(1): 85. <https://doi.org/10.1186/s12969-023-00872-1>
  29. XIONG L-J, TONG Y, WANG Z-L, MAO M: Is Helicobacter pylori infection associated with Henoch-Schönlein purpura in Chinese children? a meta-analysis. *World J Pediatr* 2012; 8(4): 301-8. <https://doi.org/10.1007/s12519-012-0373-1>
  30. WANG Z, LAI Z, ZHANG X *et al.*: Altered gut microbiome compositions are associated with the severity of asthma. *J Thorac Dis* 2021; 13(7): 4322-38. <https://doi.org/10.21037/jtd-20-2189>
  31. KIM MH, RHO M, CHOI JP *et al.*: A metagenomic analysis provides a culture-independent pathogen detection for atopic dermatitis. *Allergy Asthma Immunol Res* 2017; 9(5): 453-61. <https://doi.org/10.4168/aaair.2017.9.5.453>
  32. TSURUGA K, WATANABE S, OKI E *et al.*: Imbalance towards Th1 pathway predominance in purpura nephritis with proteinuria. *Pediatr Nephrol* 2011; 26(12): 2253-58. <https://doi.org/10.1007/s00467-011-1996-5>
  33. LI Y-Y, LI C-R, WANG G-B, YANG J, ZU Y: Investigation of the change in CD4<sup>+</sup> T cell subset in children with Henoch-Schönlein purpura. *Rheumatol Int* 2012; 32(12): 3785-92. <https://doi.org/10.1007/s00296-011-2266-3>
  34. SUN D-Q, ZHANG Q-Y, DONG Z-Y, BAI F: [Levels of IL-12 produced by dendritic cells and changes of TH1/TH2 balance in children with Henoch-Schönlein purpura]. *Zhongguo Dang Dai Er Ke Za Zhi* 2006; 8(4): 307-10.
  35. WILLIAMS BL, HORNIG M, PAREKH T, LIPKIN WI: Application of novel PCR-based methods for detection, quantitation, and phylogenetic characterization of Sutterella species in intestinal biopsy samples from children with autism and gastrointestinal disturbances. *mBio* 2012; 3(1): e00261-11. <https://doi.org/10.1128/mBio.00261-11>
  36. KAAKOUSH NO: Sutterella species, IgA-degrading bacteria in ulcerative colitis. *Trends Microbiol* 2020; 28(7): 519-22. <https://doi.org/10.1016/j.tim.2020.02.018>
  37. MOON C, BALDRIDGE MT, WALLACE MA *et al.*: Vertically transmitted faecal IgA levels determine extra-chromosomal phenotypic variation. *Nature* 2015; 521(7550): 90-93. <https://doi.org/10.1038/nature14139>
  38. TREPPO E, MONTI S, DELVINO P *et al.*: Systemic vasculitis: one year in review 2024. *Clin Exp Rheumatol* 2024; 42(4): 771-81. <https://doi.org/10.55563/clinexprheumatol/gkve60>
  39. MORETTI M, TREPPO E, MONTI S *et al.*: Systemic vasculitis: one year in review 2023. *Clin Exp Rheumatol* 2023; 41(4): 765-73. <https://doi.org/10.55563/clinexprheumatol/zf4daj>
  40. PETROU D, KALOGEROPOULOS P, LLIAPIS G, LIONAKI S: IgA nephropathy: current treatment and new insights. *Antibodies* (Basel) 2023; 12(2): 40. <https://doi.org/10.3390/antib12020040>
  41. MARTÍNEZ-LÓPEZ M, IBORRA S, CONDE-GARROSA R *et al.*: Microbiota sensing by Mincle-Syk axis in dendritic cells regulates interleukin-17 and -22 production and promotes intestinal barrier integrity. *Immunity* 2019; 50(2): 446-61.e9. <https://doi.org/10.1016/j.immuni.2018.12.020>
  42. HUANG X, YANG W, YAO S *et al.*: IL-21 promotes intestinal memory IgA responses. *J Immunol* 2020; 205(7): 1944-52. <https://doi.org/10.4049/jimmunol.1900766>
  43. CAO AT, YAO S, GONG B, NURIEVA RI, ELSON CO, CONG Y: Interleukin (IL)-21 promotes intestinal IgA response to microbiota. *Mu-*

- cosal Immunol* 2015; 8(5): 1072-82. <https://doi.org/10.1038/mi.2014.134>
44. PILLEBOUT E, JAMIN A, AYARI H *et al.*: Biomarkers of IgA vasculitis nephritis in children. *PLoS One* 2017; 12(11): e0188718. <https://doi.org/10.1371/journal.pone.0188718>
45. KIMURA S, TAKEUCHI S, SOMA Y, KAWAKAMI T: Raised serum levels of interleukins 6 and 8 and antiphospholipid antibodies in an adult patient with Henoch-Schönlein purpura. *Clin Exp Dermatol* 2013; 38(7): 730-36. <https://doi.org/10.1111/ced.12089>
46. YUAN L, WANG Q, ZHANG S, ZHANG L: Correlation between serum inflammatory factors TNF- $\alpha$ , IL-8, IL-10 and Henoch-Schönlein purpura with renal function impairment. *Exp Ther Med* 2018; 15(4): 3924-28. <https://doi.org/10.3892/etm.2018.5876>
47. WU H, WEN Y, YUE C, LI X, GAO R: Serum TNF- $\alpha$  level is associated with disease severity in adult patients with immunoglobulin A vasculitis nephritis. *Dis Markers* 2020; 2020: 5514145. <https://doi.org/10.1155/2020/5514145>
48. CAO AT, YAO S, GONG B, ELSON CO, CONG Y: Th17 cells upregulate polymeric Ig receptor and intestinal IgA and contribute to intestinal homeostasis. *J Immunol* 2012; 189(9): 4666-73. <https://doi.org/10.4049/jimmunol.1200955>
49. AL-SADI R, BOIVIN M, MA T: Mechanism of cytokine modulation of epithelial tight junction barrier. *Front Biosci (Landmark Ed)* 2009; 14(7): 2765-78. <https://doi.org/10.2741/3413>
50. LI F, HAN Y, CAI X *et al.*: Dietary resveratrol attenuated colitis and modulated gut microbiota in dextran sulfate sodium-treated mice. *Food Funct* 2020; 11(1): 1063-73. <https://doi.org/10.1039/c9fo01519a>
51. JUNG Y, WEN T, MINGLER MK *et al.*: IL-1 $\beta$  in eosinophil-mediated small intestinal homeostasis and IgA production. *Mucosal Immunol* 2015; 8(4): 930-42. <https://doi.org/10.1038/mi.2014.123>
52. NOVAL RIVAS M, WAKITA D, FRANKLIN MK *et al.*: Intestinal permeability and IgA provoke immune vasculitis linked to cardiovascular inflammation. *Immunity* 2019; 51(3): 508-21. <https://doi.org/10.1016/j.immuni.2019.05.021>
53. CHEN A, SHEU LF, CHOU WY *et al.*: Interleukin-1 receptor antagonist modulates the progression of a spontaneously occurring IgA nephropathy in mice. *Am J Kidney Dis* 1997; 30(5): 693-702. [https://doi.org/10.1016/s0272-6386\(97\)90495-9](https://doi.org/10.1016/s0272-6386(97)90495-9)